Nonlinear Processes in Geophysics (2000) 7: 191–200

Nonlinear Processes in Geophysics

Magnetic holes in the solar wind between 0.3 AU and 17 AU

K. Sperveslage[1], F. M. Neubauer[1], K. Baumgärtel[2], and N. F. Ness[3]

[1]Institut für Geophysik und Meteorologie, Universität zu Köln, D-50923 Köln, Germany
[2]Astrophysikalisches Institut Potsdam, D-14482 Potsdam, Germany
[3]Bartol Research Foundation, University of Delaware, Newark, USA

Received: 23 November 1999 – Revised: 21 June 2000 – Accepted: 7 July 2000

Abstract. Magnetic holes (MHs) are depressions of the magnetic field magnitude. Turner et al. (1977) identified the first MHs in the solar wind and determined an occurrence rate of 1.5 MHs/d. Winterhalter et al. (1994) developed an automatic identification criterion to search for MHs in Ulysses data in the solar wind between 1 AU and 5.4 AU. We adopt their criterion to expand the search to the heliocentric distances down to 0.3 AU using data from Helios 1 and 2 and up to 17 AU using data from Voyager 2. We relate our observations to two theoretical approaches which describe the so-called linear MHs in which the magnetic vector varies in magnitude rather than direction. Therefore we focus on such linear MHs with a directional change less than 10°. With our observations of about 850 MHs we present the following results: Approximately 30% of all the identified MHs are linear. The maximum angle between the initial magnetic field vector and any vector inside the MH is 20° in average and shows a weak relation to the depth of the MHs. The angle between the initial magnetic field and the minimum variance direction of those structures is large and very probably close to 90°. The MHs are placed in a high β environment even though the average solar wind shows a smaller β. The widths decrease from about 50 proton inertial length in a region between 0.3 AU and 0.4 AU heliocentric distance to about 15 proton inertial length at distances larger than 10 AU. This quantity is correlated with the β of the MH environments with respect to the heliocentric distance. There is a clear preference for the occurrence of depressions instead of compressions. We discuss these results with regard to the main theories of MHs, the mirror instability and the alternative soliton approach. Although our observational results are more consistent with the soliton theory we favor a combination of both. MHs might be the remnants of initial mirror mode structures which can be described as solitons during the main part of their lifetime.

Correspondence to: K. Sperveslage

1 Introduction

Turner et al. (1977) identified localized depressions in the magnitude of the magnetic field ($|\mathbf{B}|$) and named them magnetic holes (MHs). Using data of Explorer 43 at 1 AU, they found 28 MHs with the criterion $|\mathbf{B}| < 1$ nT which is a low intensity compared to the average intensity of 6 nT. Most of them were isolated dips embedded in a background of otherwise uniform fields. They determined an occurrence rate of 1.5 MHs/d. The widths of those MHs varied between 2 and 130 s with a median of 50 s. Their thickness along the solar radial direction was of the order of $2 \cdot 10^4$ km, corresponding to $\approx$ 200 proton gyro radii. Turner et al. (1977) defined linear holes by no or little directional change and observed them in regions of high proton β. The linear MHs were related to diamagnetic effects due to the presence of localized plasma inhomogeneities, the origin of which was not explained by the authors (Turner et al., 1977).

More recently Winterhalter et al. (1994) published a comprehensive study of MHs in the undisturbed solar wind between 1 AU and 5.4 AU up to −23° solar latitude. They used Ulysses data to identify MHs with a more general criterion in an automated search procedure. After Turner et al. (1977) had presented a few examples of linear MHs, Winterhalter et al. (1994) found in the larger time interval of 26 months about 4000 magnetic depressions. These were not only isolated but also closely spaced dips in a noisy background field. The occurrence rate was higher than, and the average width was similar to the observations of Turner et al. (1977). Approximately 30% of all MHs were linear with a directional change less than 5°. In order to investigate the generation mechanism they checked the conditions for the mirror instability. Discarding an electron pres-

sure anisotropy a plasma is unstable against this instability if β_i, the quotient of the ion plasma to the magnetic pressure, is larger than one and if there is a sufficiently strong temperature anisotropy of plasma ions ($T_\perp/T_\parallel > 1$) (Hasegawa, 1969). Winterhalter et al. (1994) confirmed that the solar wind in general is stable against it where they also neglected possible electron pressure anisotropy. However, the local environment of the MHs exhibited higher values of β_i and the ion temperature anisotropy as well so that the conditions were close to satisfied. The plasma containing trains of closely spaced holes was closer to mirror instability than the plasma containing isolated ones. An important argument for the identification of mirror mode structures is an anticorrelation of the magnetic field magnitude and the density, which was fulfilled for the small subset of MHs for which plasma measurements inside the hole were available. The authors concluded that the observed linear magnetic holes were probably remnants of structures caused by the occasional mirror instability in the solar wind.

Beside these observations of MHs in the solar wind, similar features are found near the comet Halley (Russell et al., 1987) and in planetary magnetosheaths, which are favored regions for magnetic field depressions. The magnetosheath of the earth was examined by Kaufmann et al. (1970) and Tsurutani et al. (1982), of Saturn by Tsurutani et al. (1982), Violante et al. (1995) and Bavassano-Cattaneo et al. (1998), and of Jupiter by Tsurutani et al. (1993) and Erdös and Balogh (1996).

Erdös and Balogh (1996) observed closely spaced dips on the passage of Ulysses through the magnetosheath of Jupiter. Although the surrounding plasma was unstable against the mirror instability there were still some difficulties to interpret these dips as mirror modes. Erdös and Balogh (1996) as well as others noted that the linear theories neither account for the asymmetry in the occurrence of depressions and compressions of the field magnitude nor for the observed large size of the individual depressions. They pointed out the importance of nonlinear effects.

Bavassano-Cattaneo et al. (1998) observed mirror mode structures in the magnetosheath of Saturn. They chose the data measured by Voyager 2 in the subsolar region so that the spacecraft trajectory was parallel to the flow lines of the plasma. Because of this special geometry, they were able to track the evolution from quasi-sinusoidal waves near the bow shock in the outer magnetosheath to non-periodic structures, consisting of both magnetic field compressions and depressions, and, finally, to dips close to the magnetopause. The dips resembled MHs introduced by Turner et al. (1977). Most of the properties of the described compressive fluctuations supported the interpretation as mirror modes. But when Bavassano-Cattaneo et al. (1998) compared their observations and the predictions of even nonlinear theories (Kivelson and Southwood, 1996) it appeared that there were still some unexplained values and variations, e.g. the width of the mirror structures.

In this study we examine linear MHs in the solar wind using the data of the missions Helios 1 and 2 and Voyager 2. With the covered region from 0.3 AU to 17 AU we supplement the study of Winterhalter et al. (1994) who observed MHs between 1 AU and 5.4 AU. While our data have been obtained in the ecliptic plane Winterhalter et al. (1994) had to account for an additional variation of the heliocentric latitude between +5° and -23°. We use basically the same search method as Winterhalter et al. (1994), and determine similar and some further quantities and correlations, like the normal vector of the MHs. In contrast to Winterhalter et al. (1994) who related the MHs to mirror mode structures, we mainly compare our observations with the predictions of the soliton approach (Baumgärtel et al., 1997; Baumgärtel, 1999). It suggests an alternative description because of the obvious nonlinear character of MHs and the open questions in the mirror mode interpretation. Solitons are the result of a combined action of nonlinearity and dispersion of the basic system and do not need an instability to explain their nature. In this sense MHs are suggested to be representatives of a class of magnetohydrodynamic solitons which are characterized by a magnetic depression and a density increase which combine to maintain a quasi-pressure balanced structure, that propagates slowly at large angles to the ambient field.

Several measurable quantities, such as the plasma beta, are similar in plasmas carrying mirror waves or solitons. But the different simulations of mirror modes (Price et al., 1986) and solitons (Baumgärtel, 1999) predict different properties of the magnetic field depressions. We have to keep in mind the work of Pantellini (1998), who presented a model for the formation of structures like magnetic holes based on the nonlinear mirror instability. Although he provided quantitative results we do not compare those in detail with our observations because of his rather simple model with assumptions like, for example, cold electrons.

In the first step, we describe the data sets used and the criterion for the identification of MHs. Then the observations and statistical results will be presented. The interpretations related to the soliton approach and mirror modes are included in our final discussion.

2 Data sets

We use data from the three missions Helios 1 and 2 and Voyager 2. The similar orbits of Helios 1 and 2 cover heliocentric distances between 0.3 AU and 1 AU. Both satellites had an orbital period of $\approx$ 186 days, and their instrumentation was identical. The magnetometer experiment provided a highest resolution of ± 0.2 nT with a maximum sampling rate of 8 vectors/s (Musmann et al., 1975). For our investigations data with a sampling rate

of 4 vectors/s are available. The plasma experiment (Schwenn et al., 1975) consisted of three analyzers for ions with an energy range from 0.155 to 15.32 keV/q and one analyzer for electrons with an energy range from 0.5 eV/q to 1.66 keV/q. Available are the proton measurements (I1) with the maximum data resolution of 40.5 s. For our studies we choose for Helios 1 the time interval 1974, DOY 346 until 1976, DOY 365 and for Helios 2 1976, DOY 015 - 1976, DOY 125.

Concerning the data from Voyager 2, we choose the time interval 1978, DOY 001 - 1985, DOY 224 with two big gaps around the pass of Jupiter (1978, DOY 280 - 1979, DOY 365) and of Saturn (1981, DOY 225 - 1982, DOY 084). With regard to the heliocentric distance we cover the regions from 2 to 4 AU, from 6 to 8.5 AU and from 10 to 17 AU. For our investigations we use 1.92 s magnetic field averages (Behannon et al., 1977). The plasma experiment (Bridge et al., 1977) provided the velocity, density and pressure of the solar wind plasma. The energy range for protons and for electrons is from 10 to 5950 eV. Available are proton plasma parameters supplied every 96 s.

The orbit of Voyager 2 was placed close to the ecliptic, and both Helios missions were in the ecliptic plane. As Ulysses moved to higher heliocentric latitude we have to compare carefully our results with those of Winterhalter et al. (1994) who used Ulysses data. In our selected data interval Helios 1 covers equally all heliocentric distances between 0.3 and 1 AU including nearly 4 complete orbits. We use Helios 2 only for the verification of the Helios 1 results and especially for the examination of β_{total}. Because the temperature of electrons entering the computation is only available for an interval of 110 days the selected data interval for Helios 2 has the same length. The Helios 2 interval is mainly placed near the perihelion between 0.3 and 0.4 AU. Therefore we concentrate on the presentation on Helios 1. Compared with the large difference between the results of Voyager 2 and the results of both Helios missions, the results of Helios 1 and 2 are very similar. We have to note that the chosen time intervals of the different data sets are associated with different parts of the solar cycle.

3 Identification criterion

To identify MHs in the magnetic field data of the given time intervals we use the same criterion as Winterhalter et al. (1994). We repeat the method for the benefit of the readers and to point out some small deviations. The data are continuously scanned by intervals of 300 s in length. For every interval we determine the average magnetic field magnitude B_0 and the minimum value B_{min}. In case of $B_{min}/B_0 < 0.5$ this depression is registered as a magnetic hole. The start and end vector of the MH are defined as the nearest vectors to B_{min} with a magnitude $B_{start,end}$ of one standard deviation below the average field.

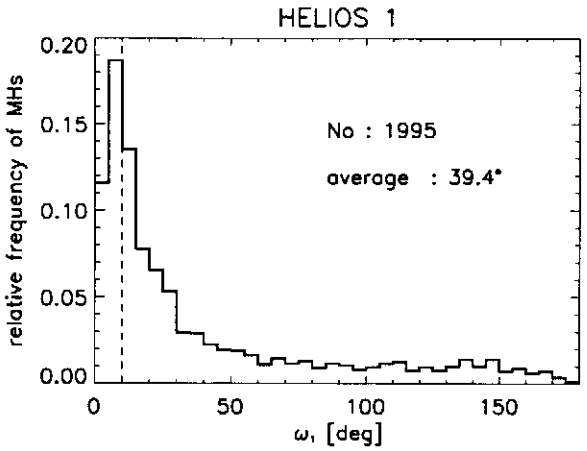

Fig. 1. Distribution of ω_1 for 1995 MHs found by Helios 1. The angle ω_1 describes the directional change between the start and the end vector of the MH. The dashed line at 10.0° marks the boundary below which a MH is classified as 'linear'.

As mentioned above, we focus our observations on the so-called linear MHs which require little or no directional change across the MH. We look for MHs with an angle ω_1 between the start and end vector of less than 10°. In the case of our three data sets about 30% of all automatically identified MHs are linear. Figure 1 shows a histogram for all events found by Helios 1 for example. Quite a large fraction of the MHs is not useful because of data gaps nearby and some noise level, for example, some remaining spin variations. After visual inspection of each MH we choose 50% and 30% out of the linear MHs for Helios 1/2 and Voyager 2, respectively. The detailed numbers are presented in Table 1.

While Winterhalter et al. (1994) used adjacent intervals of 300 s in length we add an overlap of 150 s in order to improve the detectability of MHs included in trains of closely spaced depressions. Another difference from their study is the condition for the MHs to be classified as linear. If we also require $\omega_1 < 5°$ like Winterhalter et al. (1994) instead of our $\omega_1 < 10°$ the number of the useful linear MHs would decrease from 852 to 340 that is too small for reliable statistics. We assume that this difference has no big influence on the average properties of the MHs. Winterhalter et al. (1994) defined their criterion empirically in order to identify most of the ex-

Table 1. Numbers of MHs for each mission and for different groups of MHs.

	HE 1	HE 2	VY 2	$\sum$
all MHs	1995	979	2271	5245
linear ($\omega_1 < 10°$) MHs	645	323	623	1591
linear ($\omega_1 < 10°$) useful MHs	415	186	251	852
linear ($\omega_1 < 5°$) useful MHs	164	89	87	340

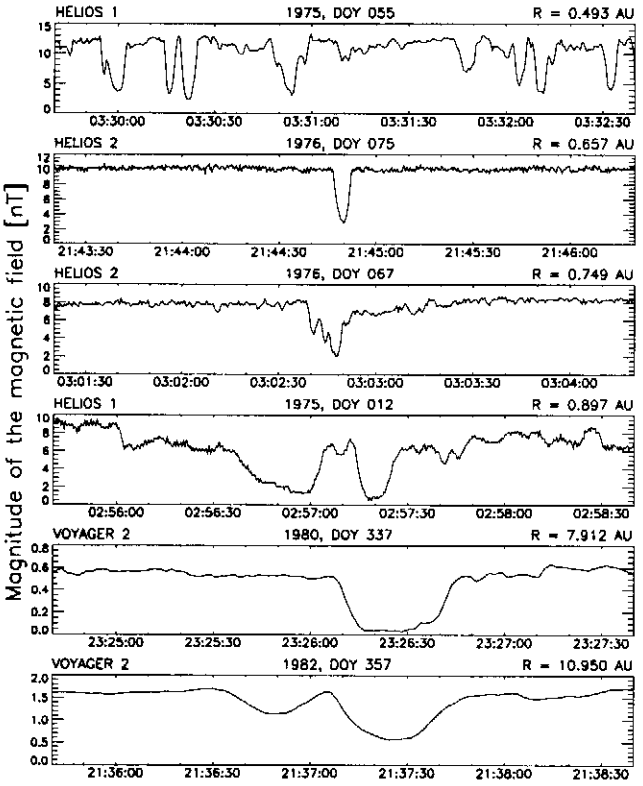

Fig. 2. Examples of magnetic holes in the highest resolution data of the missions Voyager 2 (1.92 s), Helios 1 and 2 (0.25 s); time intervals are three minutes.

isting MHs in their data set. Since these Ulysses data cover the heliocentric distances from 1 AU to 5.4 AU the criterion is valid for this kind of solar wind plasma. The upper limit of $B_{min}/B_0 = 0.5$ and the window length of 300 s would change if their approach were applied to the near-sun plasma or for the plasma beyond the Jupiter orbit.

4 Observations

The following statistics are based on 852 useful linear MHs. The observed events of the Helios missions are distributed over the heliocentric distances as well as the corresponding data sets. In contrast to the events of Helios 1 that are almost equally distributed, the events found by Helios 2 are mainly placed near the perihelion. Most of the useful linear Voyager-MHs are found between 2 and 12 AU. Only 16 out of 251 are located at $R > 12$ AU. The cause may be the lower background magnetic field which makes the satisfaction of the MH-condition $B_{min}/B_0 < 0.5$ more difficult. Some examples of MHs are shown in Figure 2. There are on one hand isolated depressions embedded in a quiet background (2nd panel), and on the other hand trains of closely spaced dips (1st panel). Between these two states exist wide depressions with a complex structure inside (3rd panel), double ones (6th panel), and cases of a noisy background including partially deep depressions (4th panel). Winterhalter et al. (1994) demonstrated a similar variety of magnetic field depressions. The difference in the MHs detected in Helios 1/2 and in Voyager 2 data is remarkable. In addition to the lower background field the Voyager-MHs are wider and have more often a flat minimum inside (5th panel). Short wave trains are rare and no series of dips, like (1st panel), are found at least by use of the criterion defined suitable to the Ulysses data. Therefore the MHs of the missions are regarded separately.

4.1 Occurrence rate

The occurrence rate of MHs for Helios 2 and Helios 1 ranges between 1.7/d and 2.2/d. In the wider region from 2 to 17 AU Voyager 2 provides a smaller occurrence rate of 0.2 MHs per day. There is no dependence on the heliocentric distance inside the region from 0.3 to 1 AU. But the rate of the MHs found by Voyager 2 shows a weak decrease with increasing heliocentric distance, from 0.5/d between 2 and 4 AU down to 0.1/d beyond 11 AU after proper consideration has been given to data gaps. Additionally, the occurrence rate decreases from the near-sun region (0.3 to 1.0 AU) to the region further away from the sun (2 to 17 AU). We note that this dependence of the occurrence rate on the heliocentric distance has to be regarded with care because of the different data sets and especially the many data gaps and relatively few events in case of Voyager 2. The mean values of $\approx$ 2/d and 0.2/d differ from the values of Turner et al. (1977) (0.4/d) and Winterhalter et al. (1994) (1/d). This is caused by the different criteria. Turner et al. (1977) used only 18 days of data to search for magnetic depressions with the conditions that $|\mathbf{B}| < 1$ nT, and ω_1 is small so that their occurrence rate is not comparable to our results. As mentioned above, the criteria of Winterhalter et al. (1994) and the ones used by us differ somewhat. The maximum angle ω_1 is the dominating factor with regard to the occurrence rate. If we calculate the occurrence rate with the condition $\omega_1 < 5°$ we obtain smaller values 0.8/d (Helios 2) and 0.9/d (Helios 1). These are very similar to the value of 1/d determined by Winterhalter et al. (1994). But the corresponding value of 0.07/d for Voyager 2 is very much smaller than the other ones. The rates of Winterhalter et al. (1994) indicate no relation to heliocentric distance or to latitude.

4.2 Asymmetry of holes and enhancements

An important point for the theory are the number of magnetic depressions in relation to the number of mag-

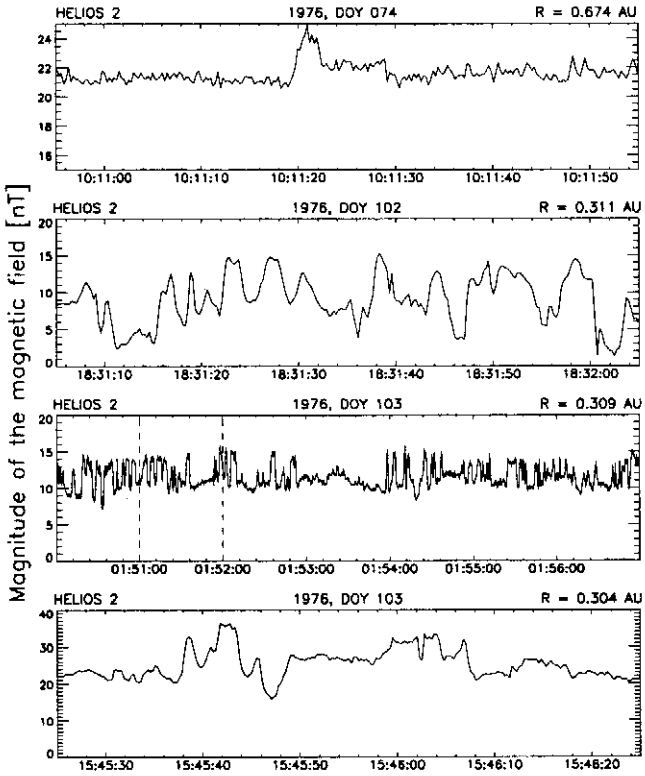

Fig. 3. Examples of magnetic enhancements in the highest resolution data of the mission Helios 2; time intervals are one minute except for panel 3.

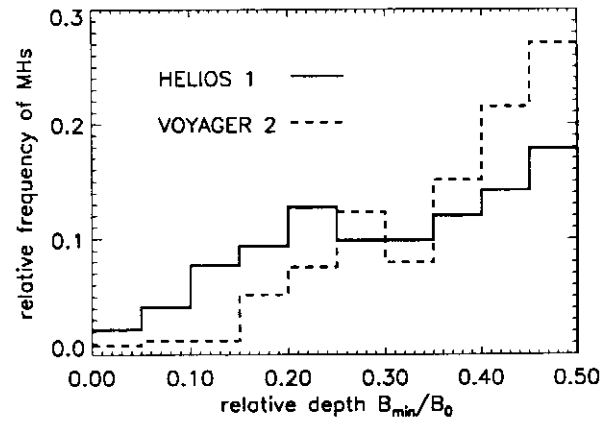

Fig. 4. Distribution of the relative depth B_{min}/B_0 for the two missions Helios 1 (solid line) and Voyager 2 (dashed line) with the bin size of 0.05.

netic compressions. We observe that holes occur much more frequently than enhancements. Even if we require $B_{max}/B_0 > 1.2$, a weaker condition than the analogue $B_{min}/B_0 < 0.5$, we do not find a significant number of magnetic enhancements. The automatic search in the data of Helios 2 provides over 2000 linear enhancements but included are a lot of various magnetic features. After a visual inspection only 26 of the 2000 events seem to be like the counterpart of a magnetic hole. Most of these few enhancements have lower amplitudes than the MHs. They are found to be either clustered or they are connected with MH-like structures. The "best" example for the few nearly isolated ones embedded in an otherwise uniform magnetic field is shown in Figure 3 (1st panel). There are two cases of series of closely spaced enhancements which are both included in a train lasting several minutes (3rd panel). Most of the identified linear and "useful" enhancements are near magnetic holes or at least embedded in a noisy background magnetic field (2nd and 4th panel).

4.3 Depth of the MHs

Since the magnetic field magnitude decreases with increasing distance from the sun, the values of B_0 and the absolute depth of MHs B_{min} differ between the missions Helios 1 and Voyager 2. While the distribution of B_{min} (not shown) in case of Helios 1 has its maximum of the relative frequency of MHs at 2 nT and then a decrease of the relative frequency of MHs up to 10 nT Voyager 2 measures for all MHs $B_{min} < 1$ nT with most of them between 0.1 and 0.2 nT. In order to compare both missions we present the distributions of the relative depth B_{min}/B_0 for the MHs (Fig.4). Both histograms show the trend of an increasing number of holes with increasing B_{min}/B_0. There are 22% (Helios 1) and 50% (Voyager 2) of the MHs in the range $0.4 < B_{min}/B_0 < 0.5$ instead of 6% (Helios 1) and 2% (Voyager 2) below 0.1. The averages vary from 0.31 for Helios 1 to 0.37 for Voyager 2. Winterhalter et al. (1994) showed a comparable distribution of B_{min}.

4.4 Directional change

The angle ω_1 between the start and the end vector determines if the MH is called linear or not. As mentioned above, we restrict our examination to linear MHs, that means $\omega_1 < 10°$. The low average of about 5° for linear MHs confirms the similarity of the field before and after the MH. Since rotations inside the MH are not included in this angle we determine the real directional change ω_2 across every depression. ω_2 is the maximum angle between the start vector and any vector inside the MH. For example, the distribution of ω_2 for Helios 1 is shown in Figure 5. About 60% of the MHs exhibit values between 5 and 20°, and only for about 10% ω_2 is larger than 40°. The higher values for ω_2 of about 20° prove a rotation inside the MH in addition to the directional change between the start and the end vector. Because of the "data accuracy" only such vectors have been taken into account for which every component $|B_i|$

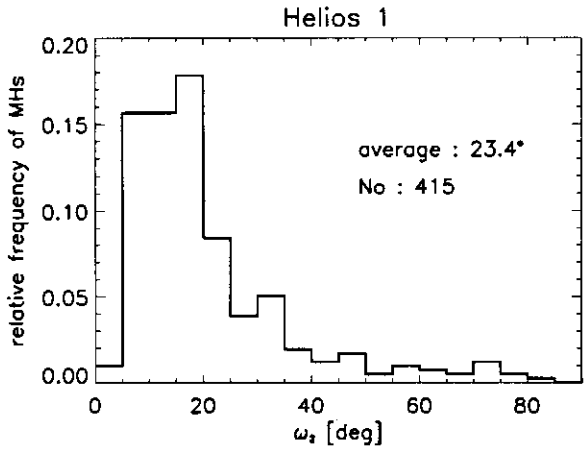

Fig. 5. Distribution of ω_2 for 415 linear MHs found by Helios 1. The angle ω_2 describes the maximum directional change between the start and any vector inside the MH. The bin size is 5.0° and the average is 23.4°.

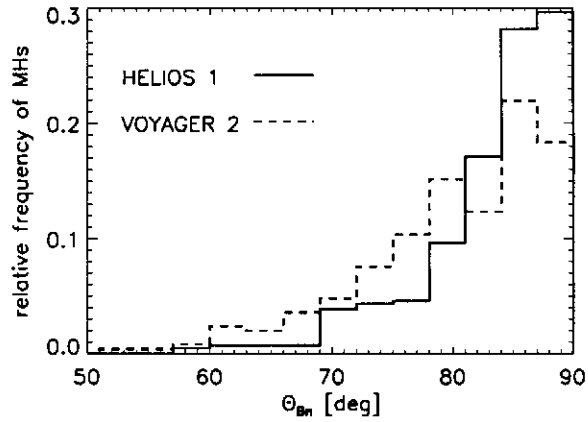

Fig. 6. Distribution of Θ_{Bn}, the angle between the minimum variance direction and the initial field vector. Plotted are the histograms for Helios 1 (solid line) and Voyager 2 (dashed line) with the bin size of 3.0°

reaches 0.2 nT. This is done for both Helios missions. In spite of some uncertainties caused by data close to zero it is clear that the magnetic field vector inside the MH rotates more than the directional change between the start and end vector leads to suppose.

4.5 Minimum variance analysis

For each MH we perform a minimum variance analysis (MVA) after Sonnerup and Cahill (1967). From the start to the end vector it includes on average 17 (Voyager 2) and 27 (Helios 1 and 2) vectors, respectively. We computed the eigenvalues and eigenvectors. The averages and medians (in brackets) of the MVA eigenvalue ratios are shown in Table 2. The minimum variance direction cannot be determined very accurately because the eigenvalue ratios are not very large in general. Therefore these results have to be regarded with care. Because of the high values for the maximum to intermediate eigenvalue ratio ($\lambda_{max}/\lambda_{int}$) compared with the lower intermediate to minimum ratios ($\lambda_{int}/\lambda_{min}$) the variance ellipsoid is cigar-shaped. This means that the magnetic field variations are more or less linear polarized in agreement with the idea of a linear MH. Additionally, we determine the angle Θ_{Bn} between the minimum variance direction and the start vector of the MHs which is close to 90° (Fig.6). In other words, the structures are aligned almost perpendicular to the magnetic field. The averages range from 80° to 85°. While in case of Helios 1 nearly 80% of the angles are larger than 80° only 50% of the MHs measured by Voyager 2 lie in this range. The average value of 83° and the distribution of Θ_{Bn} in Erdös and Balogh (1996) determined for the magnetosheath of Jupiter are similar to our results.

Table 2. The MVA results of the three missions. The averages and medians (in brackets) are given.

	HE 1	HE 2	VY 2
$\lambda_{max}/\lambda_{int}$ (median)	29.3 (16.8)	25.6 (16.0)	64.3 (36.8)
$\lambda_{int}/\lambda_{min}$ (median)	5.0 (2.7)	3.7 (2.7)	8.4 (4.7)
Θ_{Bn}[°] (median)	83.3 (85.0)	84.9 (86.2)	80.2 (83.7)

4.6 Width in different units and distances

With the determination of the start and end vector for each MH the temporal width $D_s[s]$ is given. The average duration of near-sun MHs of about 8 s and of about 32 s for MHs distributed over the region from 2 to 17 AU differ significantly. A certain part of this difference might be caused by the lower data resolution of Voyager 2 but there is in fact a physical effect. Winterhalter et al. (1994) determined for the region between 1 and 5.4 AU the most probable value lying in the 10- to 15-s bin and the median width of 22 s, which corresponds with our results. The MHs found by Voyager 2 in the interval between 2 and 4 AU show a width of 23 s on average (Fig.7). For a more detailed examination we calculate the spatial size. We use the already known minimum variance direction $\mathbf{n}$ and the actual solar wind velocity $\mathbf{v}_{sw}$ to get the width $D_{km}[km] = D_s\,\mathbf{n} \cdot \mathbf{v}_{rel}$. Because of the high velocity of about $60 - 70$ km/s for the Helios 1 and 2 spacecraft near the perihelion, the relative velocity $\mathbf{v}_{rel} = \mathbf{v}_{sw} - \mathbf{v}_{HE}$ is used. In case of Voyager 2 the lower and almost constant velocity of the spacecraft is neglected so that $\mathbf{v}_{rel} = \mathbf{v}_{sw}$. The increase of D_{km} (Fig.7, 2nd panel) with the distance R from the sun behaves as D_s (Fig.7, 1st panel). In detail, the width develops from $\approx$ 2300 km averaged over the region 0.3 to 1 AU (Helios 1) up to $\approx$ 9000 km averaged over the region 2 to 17 AU. There is also an increase

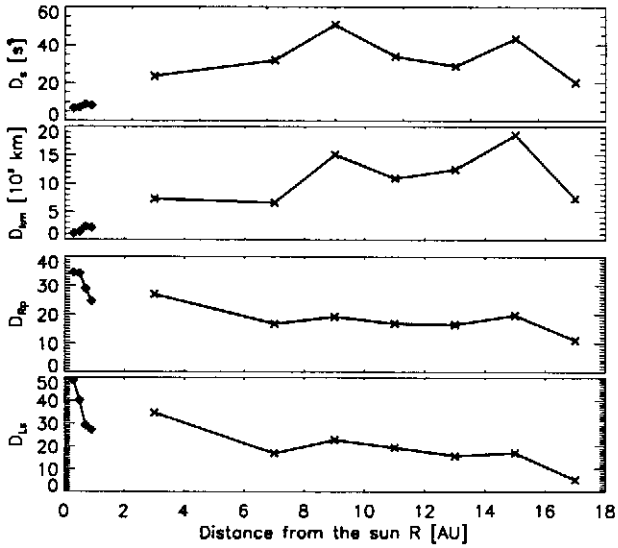

Fig. 7. Widths of MHs in different units versus the distance from the sun (s: first panel, km: second panel, proton gyro radii Rp: third panel, proton inertial length Ls: fourth panel). The values in case of Helios 1 (diamond) are averaged over 0.2 AU and 2.0 AU for Voyager 2 (cross).

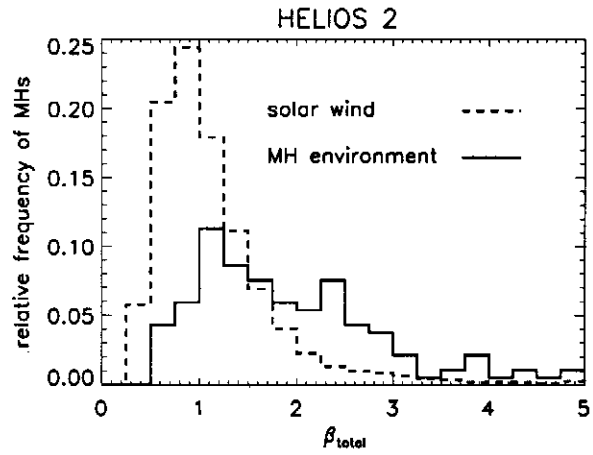

Fig. 8. Distributions of β_{total} in the MH environments (solid line) and in the average solar wind (dashed line) in case of Helios 2. The 186 MHs and 2434 hourly averages are divided in 0.25 bins.

within the near-sun interval and a weaker increase from 2 to 17 AU. In order to take into consideration the different plasma states of the distinct regions of the heliosphere we calculate normalized widths. The proton gyro radii $Rp \propto \sqrt{T} \cdot B^{-1}$ is used as a standard length, and the proton inertial length $Ls \propto (\sqrt{n})^{-1}$ which depends on the density of the plasma only is also used. Since Rp and Ls increase stronger with the heliocentric distance than the spatial size D_{km} the normalized widths $D_{Rp} = D_{km}/Rp$ and $D_{Ls} = D_{km}/Ls$ decrease from $D_{Rp} = 37$ and $D_{Ls} = 45$ averaged over 0.3 to 1 AU (Helios 1) down to $D_{Rp} = 23$ and $D_{Ls} = 27$ averaged over 2 to 17 AU, respectively. Both graphs (Fig.7, 3rd and 4th panel) are divided into a strong decrease for the Helios 1 averages and a more constant line for Voyager 2. The width in the units km, Rp and Ls depends on the minimum variance direction $\mathbf{n}$. $\mathbf{n}$ is the more confident the higher the intermediate to minimum ratio $(\lambda_{int}/\lambda_{min})$ and the larger the difference between the angle $\Theta_{\mathbf{Bn}}$ and 90°, respectively. If we consider only events with $\Theta_{\mathbf{Bn}} < 80°$ or $\lambda_{int}/\lambda_{min} > 3$ we obtain results with the same tendencies and only slightly different average values.

4.7 Plasma beta in the solar wind and the MH-environment

Most of the observed magnetic holes are located in a high β plasma. While a typical magnetosheath has a high β, the solar wind has in general lower values. We check this quantity for the MHs found by Helios 2. First, we determine the total plasma beta β_{total} in the environment of every MH. The environment is defined through the time interval from 3 minutes before the start vector until the start vector and from the end vector until 3 minutes after the end vector. While the magnetic field, proton density, and proton temperature are included in the data described above, the electron temperature is provided roughly by plots from Pilipp et al. (1990). We extract one value for each MH from their Figure 1, which allows only rough values. With the assumption that the proton density is equal to the electron density we obtain the histogram of β_{total} (Fig.8: solid line). We use their simplification because there are no data of the alpha density available.

Second, we calculate hourly averages of β_{total} of the whole time interval chosen for Helios 2 in order to describe the average solar wind. Because of the small variations of the electron temperature a constant value averaged over the 186 MH environments is used. We calculate a constant $\beta_e = 0.302$ for electrons which is added to the different β_p for protons. Finally, β_{total} contains a constant value for the electrons and varying values for protons. Both distributions of β_{total} are shown in Figure 8. There is a significant difference between the distribution of β_{total} in the solar wind (dashed line) and in the local environment of the MHs (solid line). While only 10% of the 186 MHs lie in a plasma with β_{total} less than one, this is valid for more than 50% of the average solar wind. Instead of a sharp decrease of the solar wind distribution the graph for the MH environments is more flat. With these two histograms we confirm the existence of a high β_{total} plasma in the environment of MHs in spite of lower values for the solar wind in general.

For the other missions Helios 1 and Voyager 2 no electron data were available. If we calculate and compare the distributions of the proton β_p for the two cases of solar wind and MH environments we obtain the same

trends and results as for the histograms of β_{total} in Figure 8. The only difference is a shift to lower values.

5 Discussion

In this chapter we compare our observations mainly with the predictions of the soliton theory. The idea of solitons as an explanation is rather new, and we refer to the predictions of Baumgärtel (1999). Until now the mirror instability as the underlying cause of the MHs has been favored, although both ideas are not mutually exclusive. This is because the evolution of mirror mode unstable waves into the nonlinear regime has been treated in the solar wind by Pantellini (1998) only with a simple model, whereas the soliton theory does not offer yet a source of these features. In the following we discuss selected quantities and correlations with regard to the two different theoretical approaches.

Consistent with both theoretical approaches the observed quantity β is high in the near-MH environment. The average of β_{total} is 5.4 for Helios 2 but even β_p varies from 1.6 to 2.1 for Voyager 2 and Helios 1. They are thus large enough to support the existence of the mirror instability. Baumgärtel (1999) provided stable solitons in an isotropic plasma for $1 < \beta_{total} < 5$; most of them were calculated under the assumption of $\beta = 5$. The anticorrelation of the magnitude of the magnetic field and the density is required by both theories but the time resolution of our plasma data does not admit a confirmation. Also because of a lack of data we could not verify the complete criterion for mirror mode waves involving protons and electrons (Hasegawa, 1975). Therefore we use the approach of Winterhalter et al. (1994). With the use of ion values only they concluded a state of stability for the near-MH plasma which was still stable but much closer to instability than the average solar wind. This degree of stability is not sufficient to strongly emphasize the existence of mirror waves but possibly already evolved mirror waves. For an improvement of the theory the inclusion of the nonlinearity is warranted. This is because of the high amplitudes of the observed depressions (average of $B_{min}/B_0 \approx 0.3$ in our case). The linear theory cannot explain the asymmetry between magnetic holes and enhancements that we clearly observe in the solar wind. But the nonlinear approach with respect of the mirror instability used by Kivelson and Southwood (1996) could. They considered this asymmetry but they predicted no quantitative values. Following the idea of Kivelson and Southwood (1996) Pantellini (1998) presented quantitative estimates of the characteristics of magnetic structures formed by the mirror instability. The worked out in more detail soliton approach addresses not only the asymmetry but also the nonlinear behavior. Baumgärtel (1999) used a fully nonlinear Hall-MHD system to test the stability of two possible solitary solutions, the "bright" and "dark" solitons. While the "dark" ones corresponding to magnetic holes propagate as stable entities and preserve their identity after collision, the "bright" ones (magnetic enhancements) do not exhibit the same degree of stability through the collision so that their long-time stability is questionable. This theoretical result naturally explains our large number of depressions compared with the few compressional events.

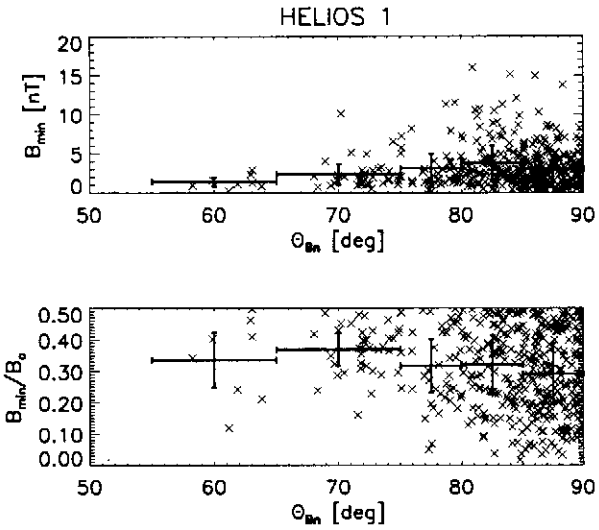

Fig. 9. B_{min}, the absolute depth of the MH (a), and B_{min}/B_0, the relative depth (b), versus Θ_{Bn}, the angle between the minimum variance direction and the initial field vector. Both plots include 415 crosses corresponding to the MHs for Helios 1 and mean values with a variable bin size and the standard deviation.

There are other quantities in which the two theoretical approaches differ. For example the angle between the minimum variance direction and the start magnetic field vector of the MHs. With the averages ranging from 80° to 85° this angle is close to perpendicular. While Baumgärtel (1999) got reasonable results by the use of $\Theta_{Bn} = 80°$ Price et al. (1986) predicted an angle between 60° and 70° in his simulations of mirror waves in the magnetosheath. Because of the uncertainty of the MVA when Θ_{Bn} is close to 90°, it is not clear whether the proposed differences are significant or not. The idea of the soliton approach predicts a relation between the angle Θ_{Bn} and the depth of the MH in the sense that the lowest magnitude of the field inside the depression that may be reached for a certain Θ_{Bn}, is proportional to $cos(\Theta_{Bn})$. Figure 9 shows the absolute depth B_{min} and the relative depth B_{min}/B_0, respectively, versus the angle Θ_{Bn}. Because no clear correlation is visible, this prediction cannot be confirmed. A similar correlation is expected with the help of ω_2, the directional change inside the MH. The larger ω_2 the deeper the MH. This implies the larger ω_2 the lower are B_{min} (Fig.10, upper panel) and B_{min}/B_0 (Fig.10, lower panel), respectively. In this sense there is a weak correlation visible so that

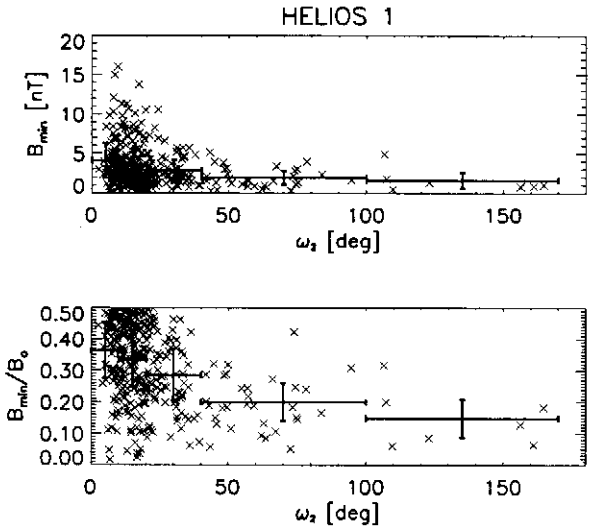

Fig. 10. B_{min}, the absolute depth of the MH (a), and B_{min}/B_0, the relative depth (b), versus ω_2. Both plots include 415 crosses corresponding to the MHs for Helios 1 and mean values with a variable bin size and the standard deviation.

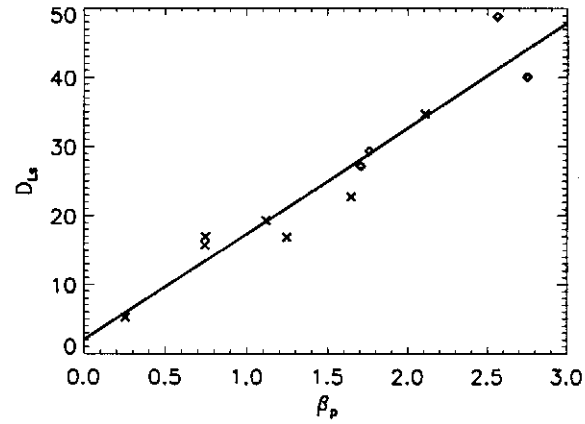

Fig. 11. The width D_{Ls} versus proton β_p. The crosses refer to the Voyager 2 results averaged over 2.0 AU, the diamonds refer to the Helios 1 results averaged over 0.2 AU.

the theoretical prediction is confirmed. A better argument for the soliton approach is the absolute value of ω_2. Instead of the low angle between the start and end vector of the magnetic depressions the observed and predicted rotation inside these structures of approximately 20° is rather large.

An interesting feature is the spatial dimension of the magnetic depressions. The predicted width from the theory of mirror mode waves by Price et al. (1986) is of the order of a few proton gyro radii only. We observe average values between 22 and 37 which is larger than the prediction. The corresponding width in units of the proton inertial length from 26 to 45 is consistent with the interval $8 < D_{Ls}/Ls < 80$ required by Baumgärtel (1999). Additionally, there is a predicted correlation between the width D_{Ls} and the value of β. Both quantities decrease with increasing heliocentric distance so that the averages over bins of the size 0.2 AU and 2.0 AU for Helios 1 and Voyager 2, respectively, fit well a line (Fig.11). Although these observations include only the β_p the predicted relation $D_{Ls} \propto \beta_{total}$ is confirmed because of the lower variations of the electron temperature.

Unfortunately, no data for the anisotropy of the temperature or the propagation velocity were available to decide between both explanations.

6 Conclusions

We have studied magnetic holes in the solar wind in a wide distance range from 0.3 AU to 17 AU heliocentric distance using the missions Voyager 2, Helios 1 and Helios 2. Using the identification criterion of Winterhalter et al. (1994) we find 852 linear magnetic holes.

Our observations of magnetic depressions with many properties, e.g. the spatial size, the angle Θ_{Bn} between $\mathbf{n}$ and $\mathbf{B}_{start}$, the directional change ω_1 and ω_2, their partial correlation with the depth, the nonlinear behavior, the asymmetry between holes and enhancements and the value of β in their environment, are in agreement with the soliton approach to magnetic holes. Although the solitons described by Baumgärtel (1999) exist without any plasma instability the mirror instability as the possible origin of MHs cannot be ruled out. While we observe not only isolated dips but also trains of closely spaced dips, Bavassano-Cattaneo et al. (1998) track the evolution of quasi-sinusoidal mirror waves to series of dips. Since they used data observed in the magnetosheath of Saturn the situation in the solar wind may be very different. If a similar evolution takes place in the undisturbed solar wind we probably would not notice it because of the difficulty to find data intervals of sufficient length on the same streamline.

Although we cannot test all predictions of the two considered theories we conclude the following. The MHs observed by us can be described by the soliton approach of Baumgärtel (1999). The variation in their appearance points to an evolution in time or space. The initial mechanism may be due to the mirror instability after some nonlinear evolution or some other nonlinear wave phenomenon.

Acknowledgements. We thank the principal investigators of the Helios and Voyager 2 plasma instruments for using their data and the data processing teams for their efforts. The work by K.S. and F.M.N. was supported financially by DARA/ DLR.

References

Baumgärtel, K., Soliton approach to magnetic holes, *J. Geophys. Res.*, *104*, 28 295+, 1999.

Baumgärtel, K., Dubinin, E., Sauer, K., and Story, T. R., Solar wind magnetic holes: Signatures of slow-mode type MHD solitons?, *Adv. Space Res.*, *20*, 69–74, 1997.

Bavassano-Cattaneo, M. B., Basile, C., Moreno, G., and Richardson, J. D., Evolution of mirror structures in the magnetosheath of Saturn from the bow shock to the magnetopause, *J. Geophys. Res.*, *103*, 11 961–11 972, 1998.

Behannon, K. W., Acuna, M. H., Burlaga, L. F., Lepping, R. P., Ness, N. F., and Neubauer, F. M., Magnetic field experiment for Voyagers 1 and 2, *Space Sci. Rev.*, *21*, 235–257, 1977.

Bridge, H. S., Belcher, J. W., Butler, R. J., Lazarus, A. J., Mavretic, A. M., and Sullivan, J. D., The plasma experiment on the 1977 Voyager mission, *Space Sci. Rev.*, *21*, 259–287, 1977.

Erdös, G. and Balogh, A., Statistical properties of mirror mode structures observed by Ulysses in the magnetosheath of Jupiter, *J. Geophys. Res.*, *101*, 1–12, 1996.

Hasegawa, A., Drift mirror instability in the magnetosphere, *Phys. Fluids*, *12*, 2642–2650, 1969.

Hasegawa, A., *Plasma Instabilities and Nonlinear Effects*, vol. 8 of *Physics and Chemistry in Space*, Springer, Berlin Heidelberg, 1975.

Kaufmann, R. J., Horng, J.-T., and Wolfe, A., Large-amplitude hydromagnetic waves in the inner magnetosheath, *J. Geophys. Res.*, *75*, 4666–4667, 1970.

Kivelson, M. G. and Southwood, D. J., Mirror instability II: The mechanism of nonlinear saturation, *J. Geophys. Res.*, *101*, 17 365–17 371, 1996.

Musmann, G., Neubauer, F. M., Maier, A., and Lammers, E., Das Förstersonden Magnetfeldexperiment (E2), *Raumfahrtforschung*, *19*, 232–236, 1975.

Pantellini, F. G. E., A model of the formation of stable nonpropagating magnetic structures in the solar wind based on the nonlinear mirror instability, *J. Geophys. Res.*, *103*, 4789–4798, 1998.

Pilipp, W. G., Miggenrieder, H., Mühlhäuser, K.-H., Rosenbauer, H., and Schwenn, R., Large-scale variations of thermal electron parameters in the solar wind between 0.3 and 1 AU, *J. Geophys. Res.*, *95*, 6305–6329, 1990.

Price, C. P., Swift, D. W., and Lee, L. C., Numerical simulations of nonoscillatory waves at the Earth's magnetosheath, *J. Geophys. Res.*, *91*, 101–112, 1986.

Russell, C. T., Riedler, C. T., Schwingenschuh, K., and Yeroshenko, Y., Mirror instability in the magnetosphere of comet Halley, *Geophys. Res. Lett.*, *14*, 644–647, 1987.

Schwenn, R., Rosenbauer, H., and Middenrieder, H., Das Plasmaexperiment auf HELIOS (E1), *Raumfahrtforschung*, *19*, 226–232, 1975.

Sonnerup, B. U. Ö. and Cahill, L. J., Magnetopause structure and attitude from Explorer 12 observations, *J. Geophys. Res.*, *72*, 171–183, 1967.

Tsurutani, B. T., Smith, E. J., Anderson, R. R., Ogilvie, K. W., Scuder, J. D., Baker, D. N., and Bame, S. J., Lion roars and nonoscillatory drift mirror waves in the magnetosheath, *J. Geophys. Res.*, *87*, 6060–6072, 1982.

Tsurutani, B. T., Southwood, D., Smith, E. J., and Balogh, A., A survey of low-frequency waves at Jupiter: The Ulysses encounter, *J. Geophys. Res.*, *98*, 21 203–21 217, 1993.

Turner, J. M., Burlaga, L. F., Ness, N. F., and Lemaire, J. F., Magnetic holes in the solar wind, *J. Geophys. Res.*, *82*, 1921–1924, 1977.

Violante, L., Bavassano-Cattaneo, M. B., Moreno, G., and Richardson, J. D., Observations of mirror waves and plasma depletion layer upstream of Saturn's magnetopause, *J. Geophys. Res.*, *100*, 12 047–12 055, 1995.

Winterhalter, D., Neugebauer, M., Goldstein, B. E., Smith, E. J., Bame, S. J., and Balogh, A., Ulysses field and plasma observations of magnetic holes in the solar wind and their relation to mirror-mode structures, *J. Geophys. Res.*, *99*, 371–381, 1994.